Journal of Applied Engineering Mathematics

Volume 10, December 2023

Modeling a Cymbal as an Annular Plate

Jacob Child and Brooke Lillie

Mechanical Engineering Department
Brigham Young University
Provo, Utah 84602
blillie98@gmail.com childjacob2@gmail.com

ABSTRACT

The purpose of this paper is to display a cymbal or other annular plate with a wave emanating from an impulse point source that is not at the boundary. This is achieved through the application of a circular integral transform, a series of Hankel transforms, and a laplace transform, with finite inverse Hankel transforms for the dirichlet-robin boundaries. The annular plate with dirichlet-robin boundaries was chosen to see if it gives a more accurate representation of a cymbal over a simple circular plate.

KEYWORDS

Cymbal, Annular Disc, Wave Equation, Circular Integral Transform, Hankel Transform, Laplace Transform, Vibrations, Animation

INTRODUCTION

The goal of this paper is to model a cymbal as an annular plate, rather than a circular plate. Other models of cymbals display the cymbal as one complete, flat, circular plate, while true cymbals consist of a flat or slightly curved disc called the surface or body, a curved center called the bell, and a small hole in the center, through which they are mounted on a stand[1]. The modeling of the cymbal as an annular plate will produce a more accurate model of the body of the cymbal, although it does not address the curved shape of the bell at the center. The visualizations and solutions can be treated as similar to, but not representative of, the real world in that the way the waves travel in the cymbal is similar to reality, but the amplitude, speed and exact patterns will likely differ.

Note: The results of this paper are highly visual and the reader is recommended to visit the link in the appendix to view the associated animations for better visualization.

EQUATION DERIVATION

Wave Equation:

The model begins with the wave equation in circular coordinates. In this equation, gamma and w are constants. Both gamma and w were assigned values of 1 in the modeling of the equation.

$$\frac{1}{r}\frac{\partial}{\partial r}\left(r\frac{\partial u}{\partial r}\right)+\frac{1}{r^2}\frac{\partial^2 u}{\partial\theta^2}+S=\frac{1}{w^2}\left(\frac{\partial^2 u}{\partial t^2}+2\gamma\frac{\partial u}{\partial t}\right)$$ [2]

The term S represents the impulse source, where the wave originates. The constants r_0 and θ_0 represent coordinates of the source of the wave function, and t_0 implies the time at which the wave starts. S_0 is another constant that gives magnitude to the point source. S_0 was assigned the value of 0.5. The points r_0, t_0, and θ_0 were assigned values of 0.5, 0, and 0, respectively.

$$S = S_0\frac{\delta\left(r-r_0\right)}{2\pi r}\,\delta\left(\theta-\theta_0\right)\delta\left(t-t_o\right)$$ [2]

Boundary Condition:

Boundary conditions are set with Dirichlet (fixed) at the inner radius, and Robin (free) at the outer radius, to represent the center being mounted on a stand, with the outside free to move. Boundaries with respect to θ are free. H_1 is a constant, with assigned value 2.

$$u_{(r_1,\theta,t)} = 0$$

$$H_1\,u_{(r_2,\theta,t)}+\frac{\partial}{\partial r}u_{(r_2,\theta,t)} = 0$$

Initial Conditions:

Initial conditions are set to 0 at t=0, such that the surface is flat at the initial time.

$$u_{(r,\theta,0)} = 0$$

$$\frac{\partial}{\partial t}u_{(r,\theta,0)} = 0$$

Integral Transforms:

With the boundaries and conditions defined, the equation is then transformed with several integral transforms, following the procedures in chapter 9 of Applied Engineering Mathematics[2]. Beginning with the circular integral transform gives the equation in terms "n".

$$\Phi_n\{\ \} = w^2\left[\frac{1}{r}\frac{\partial}{\partial r}\left(r\frac{\partial \bar{u}_n}{\partial r}\right)\right] + w^2\bar{S}_n = \frac{\partial^2 \bar{u}_n}{\partial t^2} + 2\gamma\frac{\partial \bar{u}_n}{\partial t} \quad [2]$$

In this equation $\hat{S}_n$ is given by the equation below.

$$\bar{S}_n = S_0\frac{\delta(r-r_0)}{2\pi r}\delta(t-t_0)\cos\left[n(\theta-\theta_0)\right] \quad [2]$$

The Hankel transforms are taken after the circular integral transform, and must be solved at each term "n". This results in a transformed equation with terms "n", and eigenvalues of terms "m" for each transform of term "n".

$$\mathcal{H}_n^{I-III}\{\ \} = -w^2\lambda^2_{n,m}\bar{\bar{u}}_{n,m} + w^2\bar{\bar{S}}_{n,m} = \frac{\partial^2 \bar{\bar{u}}_{n,m}}{\partial t^2} + 2\gamma\frac{\partial \bar{\bar{u}}_{n,m}}{\partial t}$$
[2]

$$\bar{\bar{S}}_{n,m} = S_0\frac{J_o(\lambda_{n,m}r_0)}{2\pi}\delta(t-t_0)\cos\left[n(\theta-\theta_0)\right] \quad [2]$$

The eigenvalues calculated for the Hankel transforms are derived from the Dirichlet-Robin boundary conditions[3]. The eigenvalue equation is set to zero and solved for values of $\lambda_{n,m}$ at each eigenvalue equation of term "n".

$$J_n(\lambda r_1)\left[-\lambda Y_{n+1}(\lambda r_2) + \left(H_1 + \frac{n}{r_2}\right)Y_n(\lambda r_2)\right] - Y_n(\lambda r_1)\left[-\lambda J_{n+1}(\lambda r_2) + \left(H_1 - \frac{n}{r_2}\right)J_n(\lambda r_2)\right] = 0 \quad [3]$$

The last transform to be done is the Laplace transform, which transforms the variable for time such that we can rearrange the equation and solve the for $U_{n,m}$.

$$\mathcal{L}\{\bar{\bar{u}}_{n,m}\} = U_{n,m} = w^2 S_0\frac{J_n(\lambda_{n,m}r_0)\cos\left[n(\theta-\theta_0)\right]}{2\pi b}e^{-\gamma(t-t_0)}\frac{b}{(s-\gamma)^2+b^2} \quad [2]$$

$$b^2 = w^2\lambda^2_{n,m} - \gamma^2$$

Inverse Transforms and Solution:

After transforming the equations the inverse finite integral transforms are taken to return $U_{n,m}$ to u.

$$u(r,\theta,t) = \frac{1}{2\pi}\hat{u}_0(r,\theta,t) + \frac{1}{\pi}\sum_{n=1}^{\infty}\hat{u}_n(r,\theta,t) \quad [2]$$

Where $\hat{u}(r,\theta,t)$ is given by the equation below.

$$\hat{u}_n(r,\theta,t) = \sum_{m=1}^{\infty}\bar{u}_{n,m}(\theta,t)\frac{J_n(\lambda_{n,m}r)}{\|N_{n,m}\|^2} \quad [2]$$

The norm is given by a standard equation, where $R_{n,m}$ is the eigenfunction of the equation.

$$\|N_{n,m}\|^2 = \int_{r_1}^{r_2} R^2_{n,m}(r)r\,dr$$

The eigenfunction is derived from the boundary conditions, and is given below.

$$R_{n,m} = \frac{J_n(\lambda_{n,m}r)}{J_n(\lambda_{n,m}r_1)} - \frac{Y_n(\lambda_{n,m}r)}{Y_n(\lambda_{n,m}r_1)} \quad [3]$$

The last term to be defined is $\bar{u}_{n,m}(\theta,t)$. This is determined from the inverse Laplace transform.

$$\bar{u}_{n,m}(\theta,t) = \frac{w^2S_0J_n(\lambda_{n,m}r_0)\cos\left[n(\theta-\theta_0)\right]}{2\pi b}e^{-\gamma(t-t_0)} * \sin\left[b(t-t_0)\right]H_1(t-t_0) \quad [2]$$

METHODS

The solution to the equation was coded and calculated in Julia (see the appendix). It consists of an inner ($\bar{u}_{n,m}$) and outer ($\hat{u}_n$) summation. This means to calculate a single r, θ point on the plate at a point in time, the inner summation will run and then the outer summation will run and the final value is u (or amplitude) at that point. The double summation causes this problem to be quite calculation heavy. To add to the computational load, the summation over m and n (inner and outer summations) not only have unique eigenvalues for each n,m point, but also a unique eigenfunction at each n, m point. The integral of the eigenfunction also needed to be found in order to calculate the norm. The math shown above was input into code and the proper functions were created to obtain the u values for each r, θ point at any moment in time. The results were then plotted and animated. Increasing n and m create a higher resolution for the result of u, which is important for the source function. The source function occurs at a single point on the plate in a single moment of time and calculating u at low n and m values loses the resolution necessary to see that point and the resulting wave split behavior. A value of 76 was chosen for both n and m. This captures the peak and the wave direction split quite well. The code was left to run overnight (it is estimated it took 3-4hrs).

RESULTS

The results of this study were quite interesting. In the animation (see appendix) some interesting results can be seen. The initial source function causes a high amplitude wave that quickly falls and travels to both sides (t = .02s see Figure 1).

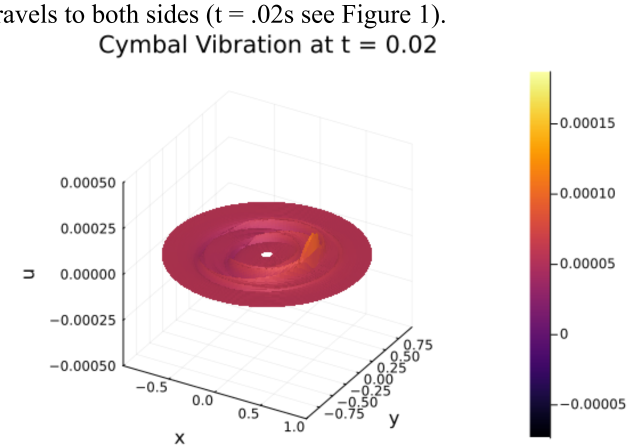

Figure 1: Just after the initial source is applied. Note: the scale is different than in Figure 2 for better visualization of the center hole.

The center of the plate is fixed, so the wave travels radially around the hole to the opposite side from the source. The amplitude is mostly negative and when the waves meet on the other side they add together and form a large negative region that pulls down that side of the plate, there is a large positive amplitude region still by the source, causing the plate to tilt (around t = .4s). The main waves continue traveling around to the other side (back towards the source) where they meet again and a negative peak forms about where the source was and a positive peak forms opposite to that (t = .89s see Figure 2).

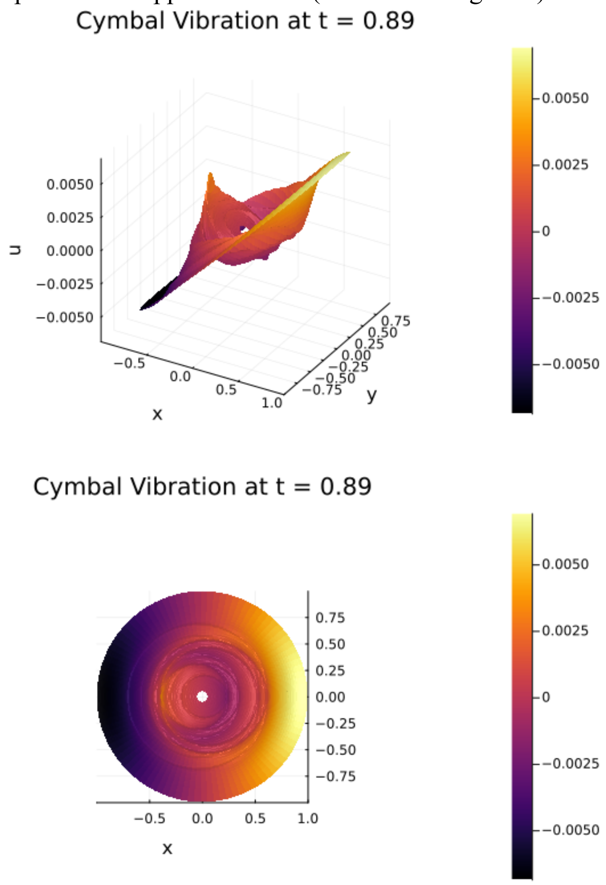

Figure 2: A side and top view of the surface at t = .89s. Note the coalescing of the waves on the side opposite of the source into a peak, and on the side of the source into a well. Shortly following this plot the plate begins to tilt back to equilibrium.

This pattern continues to repeat, for the length of the simulation. A few interesting behaviors should be noted. The "main" or peak wave seems to stay in the same general radial location around the source and appears to not travel around the center in a circular arc, but possibly in an elliptical type arc. There are simultaneously smaller amplitude waves that appear to travel radially outward from the source and reflect off of the outer edge and come back in. That edge is free, so the reflection and amplitude of the reflected wave is interesting. The very center of the annular region does stay fixed as expected and likely affects the speed at which the plate appears to recover from its tilt and stabilize horizontally. The simulation ran for two seconds and the wave amplitude as well as plate tilt oscillation amplitude were largely reduced. It is assumed that the tilting will stop relatively quickly followed eventually by the waves damping out to nothing.

CONCLUSIONS

It can be seen that the behavior of the waves in the cymbal appears to be more realistic. The waves do not travel over the center of the plate like in a real cymbal, and the plate tilts/oscillates in a manner similar to a real cymbal, as well. The unique main wave behavior traveling around the center was observed and the smaller radial waves also observed. While the amplitude and exact values and behaviors of the plate are not realistic, the general behaviors and trends are. Future work needs to be done with a non Dirichlet boundary condition on the inner radius as this will be closer to a real cymbal. Correlating the constants H, w and γ to real world parameters will also be helpful.

ACKNOWLEDGMENTS

Dr. Vladimir Soloviev for the solution to the wave equation with a cymbal as a plate and for help with Circular Integral Transforms and general math direction.
Jacob Moore For animating the cymbal as a circular plate and inspiring further research

REFERENCES

[1] Cymbal anatomy 101 (2018) Sound Pure. Available at: https://www.soundpure.com/a/expert-advice/drums/cymbal-anatomy-101/ (Accessed: 06 December 2023).
[2] Soloviev, Vladimir , Applied Engineering Mathematics, Chp 9, pg 874, https://www.et.byu.edu/~vps/ME505/IEM/09%2005%2018.pdf
[3] Soloviev, Vladimir , Applied Engineering Mathematics, Chp 7, pg 526, https://www.et.byu.edu/~vps/ME505/IEM/07%2000.pdf

APPENDIX

The source code, animations, plots, and data used can be found here (https://github.com/JacobChild/ProjectCymbal)